Amino Acids (2010) 39:111–120
DOI 10.1007/s00726-009-0382-0

ORIGINAL ARTICLE

Potential therapeutic radiotracers: preparation, biodistribution and metabolic characteristics of ^{177}Lu-labeled cyclic RGDfK dimer

Jiyun Shi · Zhaofei Liu · Bing Jia · Zilin Yu · Huiyun Zhao · Fan Wang

Received: 8 September 2009 / Accepted: 21 October 2009 / Published online: 26 November 2009

Abstract In this study, we reported the preparation and evaluation of ^{177}Lu-DOTA-RGD2, ^{177}Lu-DOTA-Bz-RGD2 and ^{177}Lu-DTPA-Bz-RGD2 (RGD2 = E[c(RGDfK)]$_2$) as a potential therapeutic radiotracers for the treatment of integrin $\alpha_v\beta_3$-positive tumors. The BALB/c nude mice bearing the U87MG human glioma xenografts were used to evaluate the biodistribution characteristics and excretion kinetics of ^{177}Lu-DOTA-RGD2, ^{177}Lu-DOTA-Bz-RGD2 and ^{177}Lu-DTPA-Bz-RGD2. It was found that there were no major differences in their lipophilicity and biodistribution characteristics, particularly at latter time points. A major advantage of using DTPA-Bz as the bifunctional chelator (BFC) was its high radiolabeling efficiency (fast and high yield radiolabeling) at room temperature. Using DOTA and DOTA-Bz as BFCs, the radiolabeling kinetics was slow, and heating at 100°C and higher DOTA-conjugate concentration were needed for successful ^{177}Lu-labeling. Therefore, DTPA-Bz is an optimal BFC for routine preparation of ^{177}Lu-labeled cyclic RGDfK peptides, and ^{177}Lu-DTPA-Bz-RGD2 is worthy of further investigation for targeted radiotherapy of integrin $\alpha_v\beta_3$-positive tumors.

Keywords Integrin $\alpha_v\beta_3$ · RGD · DTPA-Bz · ^{177}Lu · Tumor therapy

Jiyun Shi and Zhaofei Liu have contributed equally to this work

J. Shi · Z. Liu · B. Jia · Z. Yu · H. Zhao · F. Wang (✉)
Medical Isotopes Research Center, Peking University,
38# Xueyuan Road, 100191 Beijing, China
e-mail: wangfan@bjmu.edu.cn

Abbreviations

DOTA	1,4,7,10-Tetraazacyclododecane-1,4,7, 10-tetraacetic acid
DOTA-Bz	2-(*p*-Isothiocyanobenzyl)-1,4,7,10-tetraazacyclododecane-1,4,7, 10-tetraacetic acid
DTPA-Bz	2-(*p*-Isothiocyanobenzyl) diethylenetriaminepentaacetic acid

Introduction

Integrin $\alpha_v\beta_3$ plays a pivotal role in tumor angiogenesis and metastasis (Brooks et al. 1994; Folkman 2003; Jin and Varner 2004). The highly restricted expression of integrin $\alpha_v\beta_3$ in solid tumors during growth, invasion and metastasis makes it an interesting molecular target for the development of integrin $\alpha_v\beta_3$-targeted therapeutic pharmaceuticals and radiopharmaceuticals (Abdollahi et al. 2005; Alghisi and Rüegg 2006; Liu et al. 2008). In the last decade, many radiolabeled RGD-containing peptide and non-peptide antagonists have been evaluated as potential radiotracers to image the integrin $\alpha_v\beta_3$-positive tumors by positron-emission tomography or single photon-emission computed tomography (Beer et al. 2006, 2007; Chen et al. 2004; Haubner et al. 2003; Jia et al. 2006, 2008; Kenny et al. 2008; Liu et al. 2009b, 2009c). Among all the RGD peptides and analogs, [^{18}F]-AH111585 and [^{18}F]Galacto-RGD are under clinical investigations for noninvasive visualization of integrin $\alpha_v\beta_3$ expression in cancer patients (Beer et al. 2006, 2007; Haubner et al. 2003; Kenny et al. 2008). The integrin $\alpha_v\beta_3$-targeted radiotracers have been

reviewed extensively (Cai et al. 2008; Haubner et al. 2003; Liu 2006; Temming et al. 2005).

The cyclic RGDfK dimer, E[c(RGDfK)]$_2$, has been widely used as a targeting biomolecule to develop the integrin $\alpha_v\beta_3$-targeted diagnostic (^{64}Cu, ^{68}Ga, ^{18}F, ^{99m}Tc and ^{111}In) and therapeutic (^{90}Y and ^{177}Lu) radiotracers (Chen et al. 2004; Jia et al. 2006, 2008; Liu et al. 2001b, 2009b, 2009c). It was found that the radiolabeled cyclic RGD dimer had much better tumor uptake than its monomer analog due to the higher integrin $\alpha_v\beta_3$-binding affinity of E[c(RGDfK)]$_2$ than that of c(RGDfK).

Both ^{90}Y and ^{177}Lu have been used to radiolabel small biomolecules for the development of therapeutic radiopharmaceuticals (de Keizer et al. 2008; Veeravagu et al. 2008). ^{90}Y is a generator-produced radionuclide. It has a high-energy pure β^--particle emission ($E_{max} = 2.28$ MeV) with a half life of 2.7 days, which is short enough to achieve a critical radiation dose rate and at the same time is long enough to allow the radiotracer to be manufactured and delivered for clinic use. Because ^{90}Y has no γ emission, the corresponding ^{111}In-labeled compound is often used as the imaging surrogate for biodistribution and dosimetry determination (de Jong et al. 1997). ^{177}Lu is a reactor-produced radionuclide, with a half life of 6.75 days. It has three low-energy β^- emissions [$E_{max} = 0.176$ MeV (12%), 0.384 MeV (9%) and 0.497 MeV (79%)], and two γ emissions [113 keV (6.4%) and 208 keV (11%)]. Because of its low β^- energy, ^{177}Lu-labeled compounds might be useful in treating small and metastatic tumors. The presence of these two γ emissions will allow scintigraphic imaging for quantification of biodistribution and determination of radiation dosimetry in clinical settings.

As a continuation of our interest in radiolabeled cyclic RGD peptides as diagnostic and therapeutic radiotracers, we prepared the ^{177}Lu complexes (Fig. 1) of DOTA-E[c(RGDfK)]$_2$ (DOTA-RGD2), DOTA-Bz-E[c(RGDfK)]$_2$ (DOTA-Bz-RGD2) and DTPA-Bz-E[c(RGDfK)]$_2$ (DTPA-Bz-RGD2). We are particularly interested in the impact of bifunctional chelators (BFCs; DOTA, DOTA-Bz and DTPA-Bz) on biological properties (integrin $\alpha_v\beta_3$-binding affinity, biodistribution and metabolism) of the ^{177}Lu-labeled RGD2. We used BALB/c nude mice bearing the U87MG glioma xenografts to evaluate the biodistribution characteristics of ^{177}Lu-DOTA-RGD2, ^{177}Lu-DOTA-Bz-RGD2 and ^{177}Lu-DTPA-Bz-RGD2. The main objective of this study is to compare their biodistribution characteristics and excretion kinetics in the tumor-bearing mice, and to choose an optimal BFC for routine preparation of the ^{177}Lu-labeled RGD2, as well as the further therapeutic investigation of integrin $\alpha_v\beta_3$-positive tumors.

Materials and methods

General remarks

The labeling precursors, DOTA-RGD2, DOTA-Bz-RGD2 and DTPA-Bz-RGD2, were kindly provided by Dr Shuang Liu at School of Health Sciences, Purdue University. $^{177}LuCl_3$ was purchased from Perkin Elmer Life and Analytical Sciences (Boston, MA, USA). The reversed-phase C_{18} Sep-Pak cartridges were obtained from Waters (Milford, MA, USA). All buffers for radiolabeling were passed over a Chelex 100 column (Bio-Rad Laboratories, Hercules, CA, USA) (1 cm × 15 cm) to minimize trace metal contaminants. The radio-HPLC method used an HP Hewlett® Packard Series 1100 HPLC system equipped with a radiation detector (Radioflow Detector LB509) and an Agilent Zorbax SB-C18 column (4.6 mm × 250 mm, 5 μm). The flow rate was 1.0 ml/min. The mobile phase was isocratic with 90% solvent A (25 mM NaOAc buffer, pH = 5.0) and 10% solvent B (acetonitrile) at 0–2 min, followed by a gradient mobile phase going from 10% solvent B at 2 min to 30% solvent B at 10 min and to 80% solvent B at 15 min, then to 10% solvent B at 20 min. The ITLC method used Gelman-Sciences silica-gel paper strips and a 1:1 mixture of acetone and saline as the developing agent. By this method, ^{177}Lu-labeled peptide migrated to the solvent front, while free ^{177}Lu remained at the origin.

Preparation of ^{177}Lu complexes

To a clean Eppendorf tube were added 20 μl (0.5 μg/μl) of RGD dimer (DOTA-RGD2, DOTA-Bz-RGD2 or DTPA-Bz-RGD2), 180 μl of 0.2 M NaOAc buffer (pH = 5.0) and 20 μl of $^{177}LuCl_3$ solution (~5 mCi, in 0.05 N HCl). The reaction mixture was heated at 100°C for 15 ~ 20 min for the preparation of ^{177}Lu-DOTA-RGD2 or ^{177}Lu-DOTA-Bz-RGD2, while the mixture was incubated at room temperature for the preparation of ^{177}Lu-DTPA-Bz-RGD2. A sample of the resulting solution was analyzed by radio-HPLC and ITLC.

Doses preparation for animal studies

All three ^{177}Lu radiotracers were purified using Sep-Pek C-18 cartridge (Waters, MA, USA) before animal studies. To chelate the "free" ^{177}Lu, 30 μl of EDTA (6 mM, pH = 5.0) was added to the reaction mixture 5 min before purification. The Sep-Pak C-18 cartridge was activated with 10 ml of ethanol, and was washed with 10 ml of H_2O. After the Sep-Pak C-18 cartridge was loaded with radiotracer, the cartridge was then washed with 10 ml of saline to remove any ^{177}Lu-EDTA, the ^{177}Lu radiotracer was

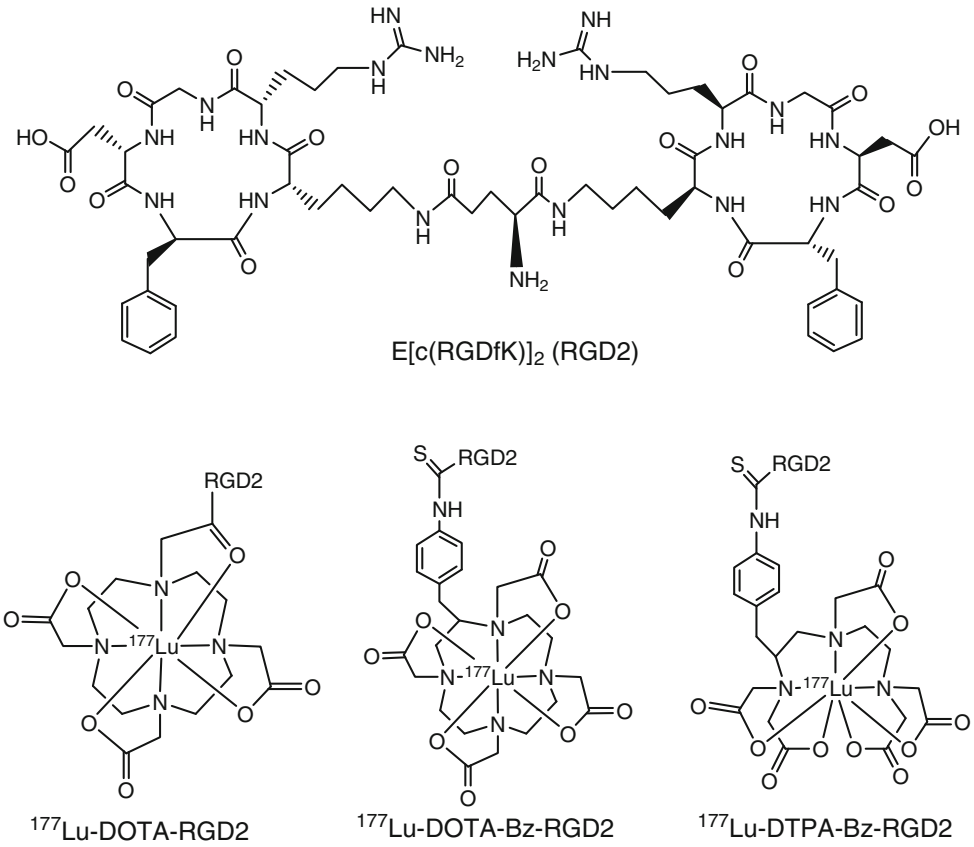

Fig. 1 Chemical structures of ^{177}Lu-DOTA-RGD2, ^{177}Lu-DOTA-Bz-RGD2 and ^{177}Lu-DTPA-Bz-RGD2 (RGD2 = E[c(EGDfK)]$_2$)

eluted with 0.4 ml of 80% ethanol. Doses for animal studies were prepared by dissolving the purified radiotracer in saline to give a concentration of 150 μCi/ml for biodistribution studies, 4.0 mCi/ml for metabolism and 2.0 mCi/ml for imaging. In the blocking experiment, excess E[c(RGDfK)]$_2$ was used as the blocking agent. Doses were prepared by dissolving excess E[c(RGDfK)]$_2$ in saline to give a final concentration of 3.0 mg/ml. Each tumor-bearing mouse was injected with 0.1 ml of solution (∼15 mg/kg).

Partition coefficients

The purified radiotracer was dissolved in a equal volume (3 ml:3 ml) mixture of *n*-octanol and 25 mM phosphate buffer (pH = 7.4). After stirring vigorously for ∼20 min, the mixture was centrifuged at 8,000 rpm for 5 min. Samples (in triplets) from *n*-octanol and aqueous layers were counted in a gamma counter (Wallac 1470-002, Perkin Elmer, Finland). The partition coefficients were calculated. The log *P* values were measured three times and reported as an average of three different measurements plus the standard deviation.

Solution stability

For the solution stability in saline, all three ^{177}Lu radiotracers were prepared, and were then purified using Sep-Pek C-18 cartridge. Samples diluted in saline were analyzed by ITLC at 2, 8, 12 and 24 h. For the solution stability in fetal bovine serum (FBS), the ^{177}Lu radiotracer was first eluted from the Sep-Pek C-18 cartridge with 0.4 ml of 80% ethanol, and then the eluate was diluted to ∼2 mCi/ml. Samples were analyzed by ITLC at 2, 8, 12 and 24 h.

Integrin $\alpha_v\beta_3$ receptor-binding assay

The in vitro integrin $\alpha_v\beta_3$-binding affinity and specificity of DOTA-RGD2, DOTA-Bz-RGD2 and DTPA-Bz-RGD2 were assessed via the competitive cell-binding assay using ^{125}I-c(RGDyK) as the receptor-specific radioligand. The ^{125}I-c(RGDyK) was prepared in a high specific activity (∼1,200 Ci/mmol) as previously described (Liu et al. 2009a, d). Receptor-binding experiments were performed on U87MG human glioma cells. The U87MG human glioma cells were maintained at 37°C and 5% CO_2 in

Dulbecco's modified Eagle's medium containing 10% FBS. In this experiment, the tumor cells were harvested, washed twice with PBS and re-suspended (2×10^6 cells/ml) in binding buffer (20 mM Tris, pH 7.4, 150 mM NaCl, 2 mM $CaCl_2$, 1 mM $MgCl_2$, 1 mM $MnCl_2$, 0.1% BSA). Filter multiscreen DV plates (96-well, pore size: 1.0 μm, Millipore, Billerica, MA, USA) were seeded with 10^5 cells/well and incubated with ^{125}I-c(RGDyK) (~200,000 cpm/well) in the presence of the increased concentrations of RGD peptide conjugates (0 ~ 1,000 nM). The total incubation volume was adjusted to 200 μl. After the cells were incubated at 4°C for 2 h, the plates were filtered through a multiscreen vacuum manifold and washed twice with cold-binding buffer. The hydrophilic PVDF filters were collected and the radioactivity was determined using a gamma counter (Wallac 1470-002, Perkin Elmer, Finland). The IC_{50} values were calculated by fitting the data by nonlinear regression using GraphPad Prism (GraphPad Software, San Diego, CA, USA). Experiments were carried out twice with triplicate samples. The IC_{50} values are reported as an average of these samples plus the standard deviation.

Biodistribution studies

All animal experiments were performed in accordance with the guidelines of Peking University Health Science Center Animal Care and Use Committee. Female BALB/c nude mice (4 ~ 5 weeks of age) were purchased from Department of Experimental Animal, Peking University Health Center. U87MG cells (5×10^6) were implanted subcutaneously into the right upper flanks of mice. When tumors reached ~0.8 cm in mean diameter, the tumor-bearing mice were used for both biodistribution and imaging studies. In short, 16 tumor-bearing mice were randomly divided into four groups, each of which had four animals. The ^{177}Lu radiotracer (15 μCi in 0.1 ml saline) was administered intravenously to each tumor-bearing mouse via tail vein. Animals were anesthetized with intraperitoneal injection of sodium pentobarbital at a dose of 45.0 mg/kg. Animals were killed by cervical dislocation at 1, 2, 4 and 24 h postinjection (p.i.). Organs were excised, washed with saline, weighed, and counted in a gamma counter (Wallac 1470-002, Perkin Elmer, Finland). Organs of interest included the tumor, blood, heart, liver, lungs, spleen, kidneys, stomach, intestine, muscle and bone. The organ uptake was calculated as a percentage of the injected dose per gram of tissue mass (%ID/g).

Blocking experiment

In the blocking experiment, the four tumor-bearing mice was administered with excess E[c(RGDfK)]$_2$ (~15 mg/kg) via tail vein about 30 min prior to the injection of ^{177}Lu-DOTA-Bz-RGD2. At 2 h p.i., all four animals were killed for organ biodistribution using the same procedure above. The results were compared with those obtained in animals without excess E[c(RGDfK)]$_2$.

Metabolism

The metabolic stability of ^{177}Lu radiotracers was evaluated in normal BALB/c nude mice. Each mouse was administered with the radiotracer (300 μCi in 0.2 ml saline) via intravenous injection. Animals were anesthetized with intraperitoneal injection of sodium pentobarbital (45.0 mg/kg). The mice were killed by cervical dislocation at 2 h p.i., and livers were removed and homogenized. The homogenate was extracted with 500 μl of 50% acetonitrile aqueous solution. The extract was centrifuged at 1,500 rpm for 15 min, and the supernatant was filtered through a 0.22-μm Millex-LG syringe driven filter unit. The filtrate was analyzed by radio-HPLC. Urine samples were collected at 2 h p.i., and were mixed with equal volume of acetonitrile. The mixtures were centrifuged at 1,500 rpm for 15 min. The supernatant was collected and filtered through a 0.22-μm Millex-LG syringe driven filter unit. The filtrate was analyzed by radio-HPLC.

Scintigraphic imaging

An imaging study was performed using three tumor-bearing mice. Each animal was administered with 400 μCi of ^{177}Lu-DOTA-Bz-RGD2 in 0.2 ml saline. Animals were anesthetized with intraperitoneal injection of sodium pentobarbital (45.0 mg/kg), then were placed supine on a two-head γ-camera (SIEMENS, E. CAM) equipped with a parallel hole, middle energy and high-resolution collimator. Anterior images were acquired at 4 h p.i., and stored digitally in a 128 × 128 matrix. The acquisition count limits were set at 200 k. Following the completion of the imaging study, animals were killed by cervical dislocation.

Statistical analysis

The biodistribution data and T/B ratios are reported as an average plus the standard deviation. Comparison between the two different radiotracers was also made using the one-way ANOVA test. The level of significance was set at $P = 0.05$.

Results

Whole-cell integrin $\alpha_v\beta_3$-binding assay

The integrin $\alpha_v\beta_3$-binding affinity of DOTA-RGD2, DOTA-Bz-RGD2 and DTPA-Bz-RGD2 was determined

using integrin $\alpha_v\beta_3$-positive U87MG human glioma cells. The integrin $\alpha_v\beta_3$-binding affinity of c(RGDyK) was also determined to demonstrate the advantage of multimer. Figure 2d shows the displacement curves of c(RGDyK), DOTA-RGD2, DOTA-Bz-RGD2 and DTPA-Bz-RGD2 against the binding of ^{125}I-c(RGDyK) to the integrin $\alpha_v\beta_3$ expressed on U87MG glioma cells. IC_{50} values were calculated to be 46.12 ± 7.49 nM for c(RGDyK), 2.35 ± 0.75 nM for DOTA-RGD2, 5.88 ± 0.35 nM for DOTA-Bz-RGD2 and 3.23 ± 0.78 nM for DTPA-Bz-RGD2.

Radiochemistry

^{177}Lu-DOTA-RGD2, ^{177}Lu-DOTA-Bz-RGD2 and ^{177}Lu-DTPA-Bz-RGD2 were prepared by reacting $^{177}LuCl_3$ with the corresponding RGDfK dimer conjugate in 200 mM NaOAc buffer (pH = 5.5). For ^{177}Lu-DTPA-Bz-RGD2, the reaction was almost instantaneous with high radiolabeling efficiency and radiochemical purity at room temperature. For ^{177}Lu-DOTA-RGD2 and ^{177}Lu-DOTA-Bz-RGD2, heating at 100°C was required to achieve high yield labeling. Under the conditions used in this study (10 μg of the cyclic RGDfK dimer conjugate for 5 mCi of ^{177}Lu), the labeling yield was >95% and the radiochemistry purity was >99% for all three ^{177}Lu radiotracers after Sep-Pek purification. Figure 2a–c shows representative radio-HPLC chromatograms for ^{177}Lu-DOTA-RGD2 (Fig. 2a), ^{177}Lu-DOTA-Bz-RGD2 (Fig. 2b) and ^{177}Lu-DTPA-Bz-RGD2 (Fig. 2c). Their log *P* values in an equal volume mixture of *n*-octanol and 25 mM phosphate buffer (pH = 7.4) were -3.39 ± 0.52, -3.47 ± 0.09 and -3.47 ± 0.26, respectively. There was no significant difference in their lipophilicity within the experimental error, which is consistent with the similarity in their HPLC retention time (Fig. 2a–c).

Solution stability

We studied solution stability of ^{177}Lu-DOTA-RGD2, ^{177}Lu-DOTA-Bz-RGD2 and ^{177}Lu-DTPA-Bz-RGD2 both in saline and in FBS (Fig. 2e, f). Low radiotracer concentration (2 mCi/ml) was used to avoid radiolytic degradation. It is clear that they all remained stable for >24 h in saline. In the FBS solution, however, ^{177}Lu-DOTA-RGD2 was stable for >24 h while ^{177}Lu-DOTA-Bz-RGD2 and ^{177}Lu-DTPA-Bz-RGD2 had 3 ~ 5% of decomposition over 24 h at room temperature.

Biodistribution characteristics

Biodistribution studies of ^{177}Lu-DOTA-RGD2, ^{177}Lu-DOTA-Bz-RGD2 and ^{177}Lu-DTPA-Bz-RGD2 were performed using the BALB/c nude mice bearing the U87MG human glioma xenografts. In general, all three radiotracers had very similar biodistribution patterns, despite their

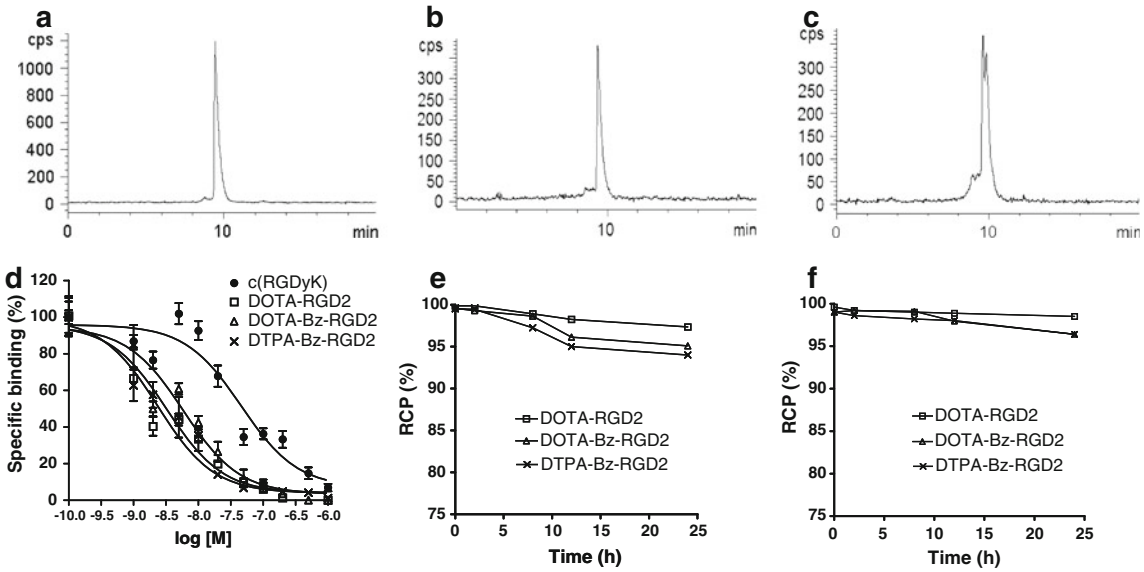

Fig. 2 Representative radio-HPLC chromatograms of ^{177}Lu-DOTA-RGD2 (**a**), ^{177}Lu-DOTA-Bz-RGD2 (**b**) and ^{177}Lu-DTPA-Bz-RGD2 (**c**); **d** in vitro inhibition of ^{125}I-c(RGDyK) binding to integrin $\alpha_v\beta_3$ on U87MG human glioma cells by c(RGDfK) (*dark filled circle*, $IC_{50} = 46.12 \pm 7.49$ nM), DOTA-RGD2 (*open square*, $IC_{50} = 2.35 \pm 0.75$ nM), DOTA-Bz-RGD2 (*open triangle*, $IC_{50} = 5.88 \pm 0.35$ nM), and DTPA-Bz-RGD2 (*cross symbol*, $IC_{50} = 3.23 \pm 0.78$ nM) (mean ± SD, $n = 3$); solution stability of ^{177}Lu-DOTA-RGD2, ^{177}Lu-DOTA-Bz-RGD2 and ^{177}Lu-DTPA-Bz-RGD2 in FBS (**e**) and in saline (**f**) (mean ± SD, $n = 3$)

differences in the ^{177}Lu chelates with respect to the molecular charge, chelator framework and donor atoms. For example, they all had low blood activity, and were excreted via both hepatobiliary and renal routes (Fig. 3a–c). As a result of the rapid blood clearance (Fig. 4a), they all showed very high tumor/blood ratios at 4 and 24 h p.i. (Fig. 3e, f). The tumor-to-nontumor ratios of the three radiotracers were almost identical at all time points examined, except for the much higher tumor/blood ratios of ^{177}Lu-DTPA-Bz-RGD2 and ^{177}Lu-DOTA-Bz-RGD2 when compared with ^{177}Lu-DOTA-RGD2 at 24 h p.i. (Fig. 3f). The tumor uptake of ^{177}Lu-DTPA-Bz-RGD2 (2.40 ± 0.49 %ID/g) at 1 h p.i. was significantly higher than that of ^{177}Lu-DOTA-RGD2 (1.69 ± 0.28 %ID/g) and ^{177}Lu-DOTA-Bz-RGD2 (1.85 ± 0.21 %ID/g) ($P < 0.05$); but this difference disappeared between 2 and 24 h p.i. (Fig. 4d). The liver uptake of ^{177}Lu-DOTA-Bz-RGD2 was lower than that of ^{177}Lu-DOTA-RGD2 and ^{177}Lu-DTPA-Bz-RGD2 at 1 h p.i., but all the three radiotracers showed similar liver uptake after 2 h p.i. (Fig. 4b). Among these three radiotracers, ^{177}Lu-DOTA-Bz-RGD2 had the lowest bone uptake (1.11 ± 0.28 %ID/g) at 1 h p.i. There was no significant difference between ^{177}Lu-DOTA-RGD2, ^{177}Lu-DOTA-Bz-RGD2 and ^{177}Lu-DTPA-Bz-RGD2 for the bone uptake between 4 and 24 h p.i. (Fig. 4c).

Integrin $\alpha_v\beta_3$ receptor specificity

We performed the blocking experiment using E[c(RGDfK)]$_2$ as the blocking agent to demonstrate tumor specificity of ^{177}Lu-DOTA-Bz-RGD2. Pre-injection of E[c(RGDfK)]$_2$ at a dose of 15 mg/kg significantly reduced its tumor uptake (Fig. 3d), suggesting that the tumor localization of ^{177}Lu-DOTA-Bz-RGD2 was indeed integrin $\alpha_v\beta_3$ mediated. However, its uptake in nontumor organs, such as intestine, liver, spleen, and stomach, was also significantly reduced, which is similar to the findings of studies with other radiolabeled RGD peptides.

Imaging study

The image study was performed using BALB/c nude mice bearing U87MG human glioma xenografts. Figure 5 illustrates a representative scintigraphic image of mice at 4 h after administration of ~400 μCi of ^{177}Lu-DOTA-Bz-RGD2. The tumor can be readily visualized. Regions of interests were drawn over each tumor and the contralateral muscles on the planar scintigraphic images. The tumor/muscle ratio was calculated to be 7.8 ± 0.2 ($n = 3$), which is consistent with that obtained from direct tissue sampling. High abdomen accumulation of the radioactivity was also found in the scintigraphic images.

Metabolic properties

We performed metabolism studies on ^{177}Lu-DOTA-RGD2, ^{177}Lu-DOTA-Bz-RGD2 and ^{177}Lu-DTPA-Bz-RGD2 using normal BALB/c nude mice. Because they were excreted from both renal and hepatobiliary routes, we analyzed the samples from the liver and urine to determine if they were able to retain their chemical integrity at 1 h p.i. Figure 6 illustrates the HPLC chromatograms of ^{177}Lu-DOTA-RGD2 (left) and ^{177}Lu-DTPA-Bz-RGD2 (right) in the kit matrix before injection (Fig. 6a), in the liver (Fig. 6b) and in the urine (Fig. 6c). The metabolic pattern of ^{177}Lu-DOTA-Bz-RGD2 is almost identical to that of ^{177}Lu-DOTA-RGD2. It is quite clear that there is no significant metabolism in both urine and liver samples at 1 h p.i.

Discussion

In 1980s, Meares' group was the first to use polyaza macrocycles as BFCs for radiolabeling of antibodies with ^{67}Cu and ^{90}Y (Moi et al. 1985), and found that macrocyclic BFCs formed ^{67}Cu and ^{90}Y chelates with high stability and kinetic inertness. Since then, many macrocyclic BFCs have been used for radiolabeling of biomolecules, including monoclonal antibodies, antibody fragments and small peptides (Deshpande et al. 1990; Peterson and Meares 1999). Macrocyclic and acyclic BFCs and their coordination chemistry with lanthanide radionuclides and other radiometals have been reviewed extensively (Blower et al. 1996; Liu 2004).

For radiolabeled antibodies, the attachment of BFCs does not disturb the tertiary structure of the polypeptide backbone; thereby, the biological and receptor-binding properties are not significantly affected. For small biomolecules (peptides and non-peptide receptor ligands), however, the metal chelate (radionuclide and BFC) contributes greatly to the overall size and molecular weight of the radiotracer. Because the biodistribution of radiotracers depend on the physical and chemical properties of both biomolecules and metal chelates, it is necessary to explore the impact of BFCs on tumor-targeting capability and biodistribution characteristics of radiotracers.

In this study, we prepared three cyclic RGDfK dimer conjugates (DOTA-RGD2, DOTA-Bz-RGD2 and DTPA-Bz-RGD2) and compared their integrin $\alpha_v\beta_3$-binding affinity in a whole-cell competition assay. It seems that DOTA-RGD2 (2.35 ± 0.75 nM) has a higher binding affinity than DOTA-Bz-RGD2 (5.88 ± 0.35 nM), but this difference is not significant within the limit of this assay. Apparently, the attachment of different chelators (DOTA, DOTA-Bz and DTPA-Bz) has little effect on integrin $\alpha_v\beta_3$-binding affinity of BFC-RGD2 conjugates. IC_{50}

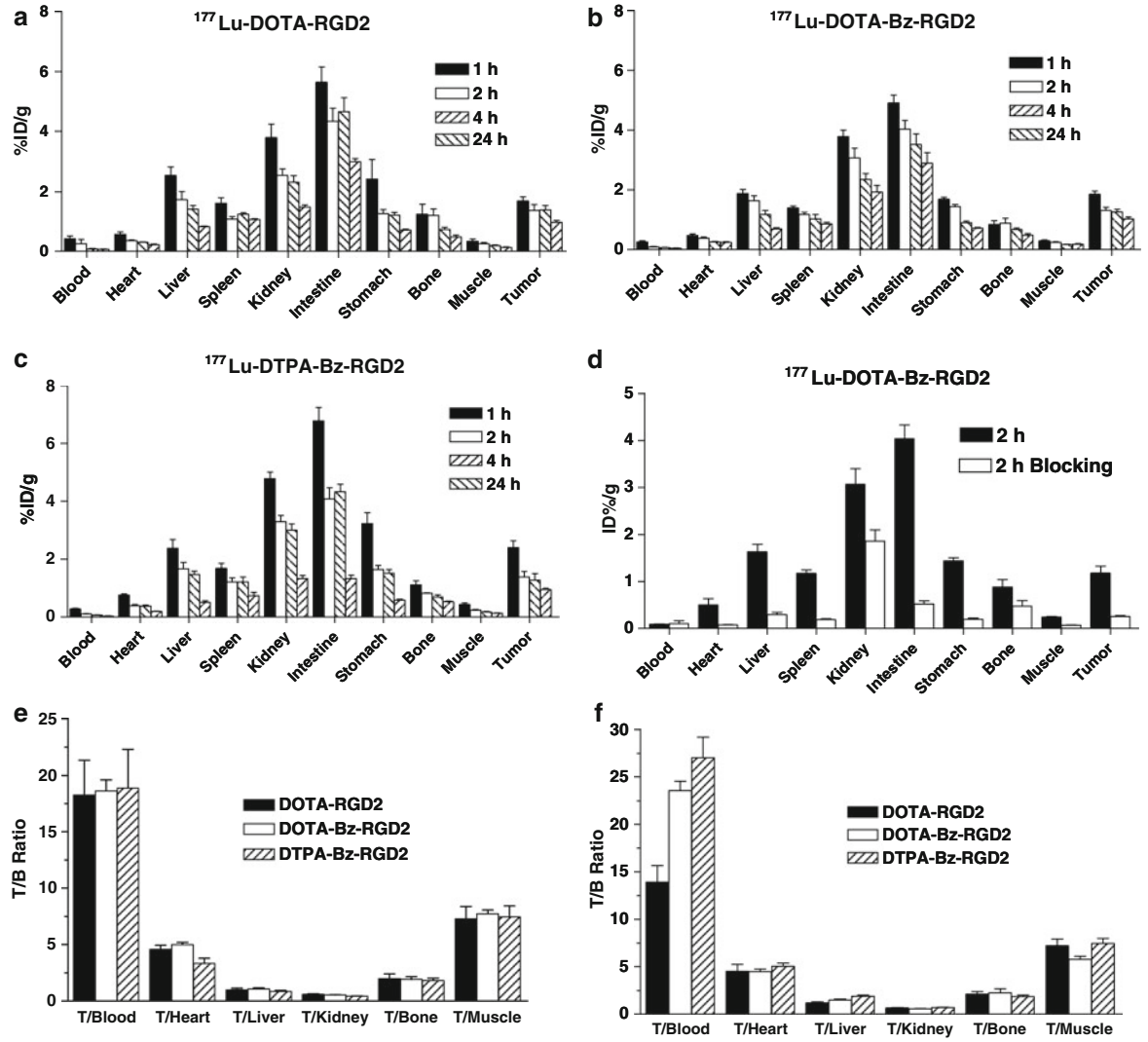

Fig. 3 Histograms of biodistribution data for ^{177}Lu-DOTA-RGD2 (**a**), ^{177}Lu-DOTA-Bz-RGD2 (**b**) and ^{177}Lu-DTPA-Bz-RGD2 (**c**) in BALB/c nude mice bearing U87MG human glioma xenografts (mean ± SD, $n = 4$ per group); biodistribution of ^{177}Lu-DOTA-Bz-RGD2 in U87MG tumor-bearing nude mice with and without coinjection of 15 mg/kg E[c(RGDfK)]$_2$ as a blocking agent at 2 h postinjection (**d**); tumor/background ratios for ^{177}Lu-DOTA-RGD2, ^{177}Lu-DOTA-Bz-RGD2 and ^{177}Lu-DTPA-Bz-RGD2 in BALB/c nude mice bearing U87MG human glioma xenografts at 4 h (**e**) and 24 h (**f**) postinjection (mean ± SD, $n = 4$ per group)

values of DOTA-RGD2, DOTA-Bz-RGD2 and DTPA-Bz-RGD2 are much lower than that of c(RGDyK) (46.12 ± 7.49 nM). Thus, formation of the cyclic RGDfK dimer increases the integrin $\alpha_v\beta_3$-binding affinity. Similar conclusions have also been made for the 6-hydrazinonicotinamide and DOTA-conjugated cyclic RGDfK dimer (Jia et al. 2006, 2008).

The difference between ^{177}Lu-DOTA-RGD2 and ^{177}Lu-DOTA-Bz-RGD2 is molecular charge. DOTA is attached to E[c(RGDfK)]$_2$ via one of four carboxylic groups. ^{177}Lu-DOTA chelate is neutral in ^{177}Lu-DOTA-RGD2. In contrast, DOTA-Bz is attached to E[c(RGDfK)]$_2$ via the isothiocyanate group, and the ^{177}Lu-DOTA-Bz chelate is anionic (Liu and Edwards 2001a). ^{177}Lu-DOTA-Bz-RGD2 is different from ^{177}Lu-DTPA-Bz-RGD2 in their ligand framework, donor atoms and molecular charge. DTPA is acyclic and contain three amine-N and five carboxylato-*O* atoms for chelation. The ^{177}Lu-DTPA chelate has two negative charges. Despite their differences in molecular charge and donor atoms, there was no significant difference in lipophilicity (log *P* values) of ^{177}Lu-DOTA-RGD2, ^{177}Lu-DOTA-Bz-RGD2 and ^{177}Lu-DTPA-Bz-RGD2, suggesting that the cyclic RGDfK dimer remains the determining factor for lipophilicity of the ^{177}Lu-labeled E[c(RGDfK)]$_2$.

The in vivo tumor targeting capability of ^{177}Lu-DOTA-RGD2, ^{177}Lu-DOTA-Bz-RGD2 and ^{177}Lu-DTPA-Bz-RGD2 was evaluated in the BALB/c nude mice bearing the U87MG human glioma xenografts. It is surprising that both biodistribution patterns (Fig. 3a–c) and excretion kinetics

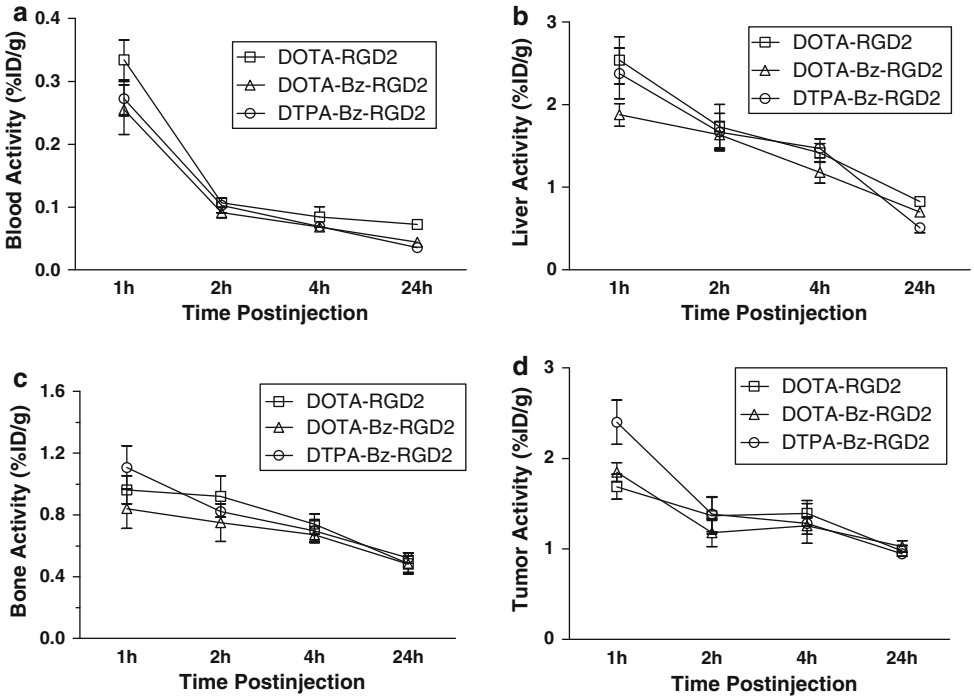

Fig. 4 Comparison of the uptake between ^{177}Lu-DOTA-RGD2, ^{177}Lu-DOTA-Bz-RGD2 and ^{177}Lu-DTPA-Bz-RGD2 in blood (**a**), liver (**b**), bone (**c**) and tumor (**d**) of BALB/c nude mice bearing U87MG human glioma xenografts (mean ± SD, $n = 4$ per group)

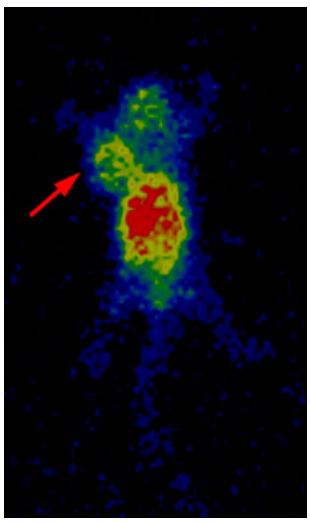

Fig. 5 A representative scintigraphic image of the tumor-bearing mice administered with ~400 μCi of ^{177}Lu-DOTA-Bz-RGD2. The *arrow* indicates the presence of tumor

(Fig. 4) of ^{177}Lu-DOTA-RGD2 and ^{177}Lu-DOTA-Bz-RGD2 are almost identical, despite the difference in molecular charge of ^{177}Lu chelates, likely caused by the presence of benzene ring in DOTA-Bz. Theoretically, the increase in negative charge in the radiometal chelate would be expected to result in the decreased lipophilicity, but this effect could be counter-balanced by the lipophilic aromatic Bz group. This may explain the similarity between ^{177}Lu-DOTA-RGD2 and ^{177}Lu-DOTA-Bz-RGD2 with respect to their log *P* values and biodistribution characteristics.

A major advantage of using DTPA analogs as BFCs is fast radiolabeling kinetics under mild conditions. Stimmel et al. studied the ^{90}Y-chelation properties of a series of DOTA and DTPA analogs (Stimmel and Kull Jr 1998; Stimmel et al. 1995). It was found that the ^{90}Y-chelation efficiency of acyclic chelators, such as DTPA and its derivatives, was much higher than that of macrocyclic chelators. The DTPA-biomolecule conjugates can be readily radiolabeled under mild conditions (room temperature and pH 4 ~ 7). Liu et al. studied the ^{90}Y-chelation kinetics of DTPA- and DOTA-conjugated small biomolecules (Liu et al. 2001a; Liu and Edwards 2001b), and found that the high yield labeling (RCP > 95%) could be readily achieved using much smaller amount of DTPA-biomolecule conjugate for the same amount of radioactivity (^{90}Y and ^{111}In), and chelation was almost instantaneous at room temperature. In contrast, the labeling kinetics of DOTA-biomolecule conjugate was very slow, and the radiolabeling yield was pretty low at room temperature. In this study, the ^{177}Lu radiolabeling of DOTA-RGD2, DOTA-Bz-RGD2 and DTPA-Bz-RGD2 was carried out at 100°C or room temperature, respectively. When compared with DOTA-RGD2 and DOTA-Bz-RGD2, the labeling kinetics of DTPA-Bz-RGD2 was much more rapid. ^{177}Lu-DTPA-Bz-RGD2 could be readily available with high labeling yield after reaction for 10 min at room temperature. In contrast, heating at 100°C was needed for the preparation of ^{177}Lu-DOTA-RGD2 or ^{177}Lu-DOTA-Bz-RGD2. The rapid reaction kinetics of ^{177}Lu-DTPA-Bz-RGD2 makes it more suitable for possible kit formulation and routine clinical application.

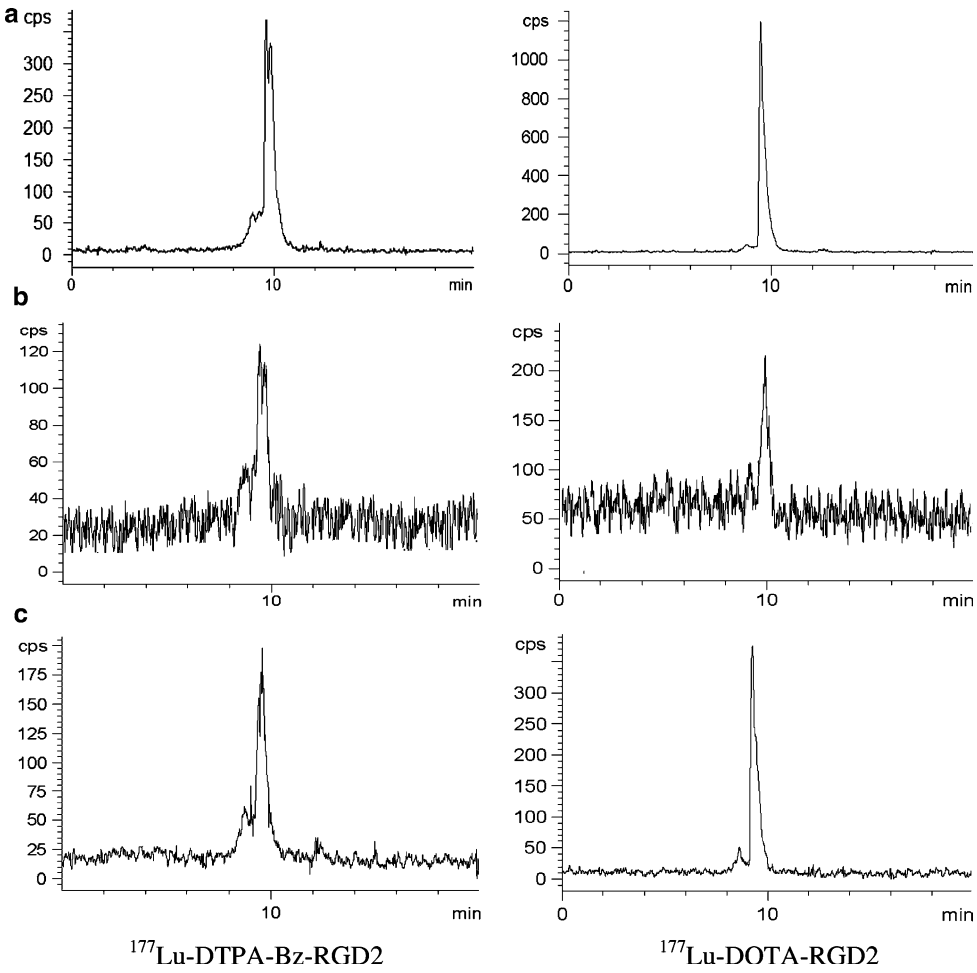

Fig. 6 Representative radio-HPLC chromatograms of ^{177}Lu-DTPA-Bz-RGD2 (*left*) and ^{177}Lu-DOTA-RGD2 (*right*) in the kit matrix (**a**), in the liver at 1 h postinjection (**b**) and in the urine (**c**) at 1 h postinjection. The metabolic stability of ^{177}Lu-DOTA-Bz-RGD2 is almost identical to that of ^{177}Lu-DOTA-RGD2. Each BALB/c mouse was administered with 300 μCi of radiotracer. Two mice were used for each radiotracer

We and other groups recently designed and synthesized several new RGD dimers with Gly_3 or PEG_4 (Gly_3 = glycine-glycine-glycine; PEG_4 = 15-amino-4,7,10,13-tetraoxapentadecanoic acid) spacers between the two RGD motifs in the homodimeric peptides (Liu et al. 2009b, 2009c; Shi et al. 2008, 2009; Wang et al. 2009). The insertion of the Gly_3 or PEG_4 spacers significantly increased the distance between the two cyclic RGD peptide motifs, resulting in an increase in vitro receptor-binding affinity. More importantly, the new ^{99m}Tc, ^{18}F and ^{68}Ga-labeled RGD dimers with Gly_3 or PEG_4 spacers exhibited significantly enhanced tumor uptake in nude mouse models (Liu et al. 2009b, 2009c; Shi et al. 2008; Wang et al. 2009). Therefore, it is also worthy of the further investigation to evaluate the tumor therapeutic efficacy of ^{177}Lu-labeled Gly_3 or PEG_4-lyted RGD dimer using DTPA-Bz as the chelator.

Conclusions

In this study, we evaluated the biodistribution characteristics and excretion kinetics of ^{177}Lu-DOTA-RGD2, ^{177}Lu-DOTA-Bz-RGD2 and ^{177}Lu-DTPA-Bz-RGD2 using BALB/c nude mice bearing U87MG human glioma xenografts. It was found that there were no major differences in their lipophilicity and biodistribution characteristics, particularly at latter time points. However, when comparing with DOTA-RGD2 and DOTA-Bz-RGD2, the ^{177}Lu labeling kinetics of DTPA-Bz was much more rapid. The easy availability, high integrin $\alpha_v\beta_3$-binding affinity/specificity, and good pharmacokinetic property of ^{177}Lu-DTPA-Bz-RGD2 make it possible for kit formulation and guarantee its further investigation for targeted therapy of integrin $\alpha_v\beta_3$-positive tumors.

Acknowledgments We thank Dr. Shuang Liu at School of Health Sciences, Purdue University, for providing radiolabeling precursors. We also thank Dr. Zhi Yang at Department of Nuclear Medicine, Peking University School of Oncology, for the friendly assistance on the animal imaging. This work is supported, in part, by NSFC projects (30640067, 30870728, 30930030 and 30900373), an 863 project (2007AA02Z467) and a Grant from the Ministry of Science and Technology of China (2009ZX09103-733).

References

Abdollahi A, Griggs DW, Zieher H, Roth A, Lipson KE, Saffrich R, Gröne H-J, Hallahan DE, Reisfeld RA, Debus J et al (2005) Inhibition of alpha(v)beta3 integrin survival signaling enhances

antiangiogenic and antitumor effects of radiotherapy. Clin Cancer Res 11(17):6270–6279

Alghisi GC, Rüegg C (2006) Vascular integrins in tumor angiogenesis: mediators and therapeutic targets. Endothelium 13(2):113–135

Beer AJ, Haubner R, Sarbia M, Goebel M, Luderschmidt S, Grosu AL, Schnell O, Niemeyer M, Kessler H, Wester HJ et al (2006) Positron emission tomography using [18F]Galacto-RGD identifies the level of integrin alpha(v)beta3 expression in man. Clin Cancer Res 12(13):3942–3949

Beer AJ, Grosu AL, Carlsen J, Kolk A, Sarbia M, Stangier I, Watzlowik P, Wester HJ, Haubner R, Schwaiger M (2007) [18F]galacto-RGD positron emission tomography for imaging of alphavbeta3 expression on the neovasculature in patients with squamous cell carcinoma of the head and neck. Clin Cancer Res 13(22 Pt 1):6610–6616

Blower PJ, Lewis JS, Zweit J (1996) Copper radionuclides and radiopharmaceuticals in nuclear medicine. Nucl Med Biol 23(8):957–980

Brooks PC, Clark RA, Cheresh DA (1994) Requirement of vascular integrin alpha v beta 3 for angiogenesis. Science 264(5158):569

Cai W, Niu G, Chen X (2008) Imaging of integrins as biomarkers for tumor angiogenesis. Curr Pharm Des 14(28):2943–2973

Chen X, Liu S, Hou Y, Tohme M, Park R, Bading JR, Conti PS (2004) MicroPET imaging of breast cancer alphav-integrin expression with 64Cu-labeled dimeric RGD peptides. Mol Imaging Biol 6(5):350–359

de Jong M, Bakker WH, Krenning EP, Breeman WA, van der Pluijm ME, Bernard BF, Visser TJ, Jermann E, Behe M, Powell P et al (1997) Yttrium-90 and indium-111 labelling, receptor binding and biodistribution of [DOTA0, d-Phe1, Tyr3]octreotide, a promising somatostatin analogue for radionuclide therapy. Eur J Nucl Med 24(4):368–371

de Keizer B, van Aken MO, Feelders RA, de Herder WW, Kam BL, van Essen M, Krenning EP, Kwekkeboom DJ (2008) Hormonal crises following receptor radionuclide therapy with the radiolabeled somatostatin analogue [177Lu-DOTA0, Tyr3]octreotate. Eur J Nucl Med Mol Imaging 35(4):749–755

Deshpande SV, DeNardo SJ, Kukis DL, Moi MK, McCall MJ, DeNardo GL, Meares CF (1990) Yttrium-90-labeled monoclonal antibody for therapy: labeling by a new macrocyclic bifunctional chelating agent. J Nucl Med 31(4):473–479

Folkman J (2003) Fundamental concepts of the angiogenic process. Curr Mol Med 3(7):643–651

Haubner RH, Wester HJ, Weber WA, Schwaiger M (2003) Radiotracer-based strategies to image angiogenesis. Q J Nucl Med 47(3):189–199

Jia B, Shi J, Yang Z, Xu B, Liu Z, Zhao H, Liu S, Wang F (2006) 99mTc-labeled cyclic RGDfK dimer: initial evaluation for SPECT imaging of glioma integrin alphavbeta3 expression. Bioconjug Chem 17(4):1069–1076

Jia B, Liu Z, Shi J, Yu Z, Yang Z, Zhao H, He Z, Liu S, Wang F (2008) Linker effects on biological properties of 111In-labeled DTPA conjugates of a cyclic RGDfK dimer. Bioconjug Chem 19(1):201–210

Jin H, Varner J (2004) Integrins: roles in cancer development and as treatment targets. Br J Cancer 90(3):561–565

Kenny LM, Coombes RC, Oulie I, Contractor KB, Miller M, Spinks TJ, McParland B, Cohen PS, Hui AM, Palmieri C et al (2008) Phase I trial of the positron-emitting Arg-Gly-Asp (RGD) peptide radioligand 18F-AH111585 in breast cancer patients. J Nucl Med 49(6):879–886

Liu S (2004) The role of coordination chemistry in the development of target-specific radiopharmaceuticals. Chem Soc Rev 33(7):445–461

Liu S (2006) Radiolabeled multimeric cyclic RGD peptides as integrin alphavbeta3 targeted radiotracers for tumor imaging. Mol Pharm 3(5):472–487

Liu S, Edwards DS (2001a) Bifunctional chelators for therapeutic lanthanide radiopharmaceuticals. Bioconjug Chem 12(1):7–34

Liu S, Edwards DS (2001b) Synthesis and characterization of two (111)In-labeled DTPA-peptide conjugates. Bioconjug Chem 12(4):630–634

Liu S, Cheung E, Rajopadhye M, Williams NE, Overoye KL, Edwards DS (2001a) Isomerism and solution dynamics of (90)Y-labeled DTPA–biomolecule conjugates. Bioconjug Chem 12(1):84–91

Liu S, Cheung E, Ziegler MC, Rajopadhye M, Edwards DS (2001b) (90)Y and (177)Lu labeling of a DOTA-conjugated vitronectin receptor antagonist useful for tumor therapy. Bioconjug Chem 12(4):559–568

Liu Z, Wang F, Chen X (2008) Integrin alpha v beta 3-targeted cancer therapy. Drug Dev Res 69(6):329–339

Liu Z, Li Z, Cao Q, Liu S, Wang F, Chen X (2009a) Small-animal PET of tumors with 64Cu-labeled RGD-bombesin heterodimer. J Nucl Med 50(7):1168–1177

Liu Z, Liu S, Wang F, Liu S, Chen X (2009b) Noninvasive imaging of tumor integrin expression using (18)F-labeled RGD dimer peptide with PEG (4) linkers. Eur J Nucl Med Mol Imaging 36(8):1296–1307

Liu Z, Niu G, Shi J, Liu S, Wang F, Liu S, Chen X (2009c) (68)Ga-labeled cyclic RGD dimers with Gly(3) and PEG (4) linkers: promising agents for tumor integrin alpha (v)beta (3) PET imaging. Eur J Nucl Med Mol Imaging 36(6):947–957

Liu Z, Yan Y, Chin FT, Wang F, Chen X (2009d) Dual integrin and gastrin-releasing peptide receptor targeted tumor imaging using 18F-labeled PEGylated RGD-bombesin heterodimer 18F-FB-PEG3-Glu-RGD-BBN. J Med Chem 52(2):425–432

Moi MK, Meares CF, McCall MJ, Cole WC, DeNardo SJ (1985) Copper chelates as probes of biological systems: stable copper complexes with a macrocyclic bifunctional chelating agent. Anal Biochem 148(1):249–253

Peterson JJ, Meares CF (1999) Enzymatic cleavage of peptide-linked radiolabels from immunoconjugates. Bioconjug Chem 10(4):553–557

Shi J, Wang L, Kim YS, Zhai S, Liu Z, Chen X, Liu S (2008) Improving tumor uptake and excretion kinetics of 99mTc-labeled cyclic arginine-glycine-aspartic (RGD) dimers with triglycine linkers. J Med Chem 51(24):7980–7990

Shi J, Kim YS, Zhai S, Liu Z, Chen X, Liu S (2009) Improving tumor uptake and pharmacokinetics of (64)Cu-labeled cyclic RGD peptide dimers with Gly(3) and PEG(4) linkers. Bioconjug Chem 20(4):750–759

Stimmel JB, Kull FC Jr (1998) Samarium-153 and lutetium-177 chelation properties of selected macrocyclic and acyclic ligands. Nucl Med Biol 25(2):117–125

Stimmel JB, Stockstill ME, Kull FC Jr (1995) Yttrium-90 chelation properties of tetraazatetraacetic acid macrocycles, diethylene-triaminepentaacetic acid analogues, and a novel terpyridine acyclic chelator. Bioconjug Chem 6(2):219–225

Temming K, Schiffelers RM, Molema G, Kok RJ (2005) RGD-based strategies for selective delivery of therapeutics and imaging agents to the tumour vasculature. Drug Resist Updat 8(6):381–402

Veeravagu A, Liu Z, Niu G, Chen K, Jia B, Cai W, Jin C, Hsu AR, Connolly AJ, Tse V et al (2008) Integrin alphavbeta3-targeted radioimmunotherapy of glioblastoma multiforme. Clin Cancer Res 14(22):7330–7339

Wang L, Shi J, Kim YS, Zhai S, Jia B, Zhao H, Liu Z, Wang F, Chen X, Liu S (2009) Improving tumor-targeting capability and pharmacokinetics of (99m)Tc-labeled cyclic RGD dimers with PEG(4) linkers. Mol Pharm 6(1):231–245